Supporting Information

McCord et al. 10.1073/pnas.1304575110

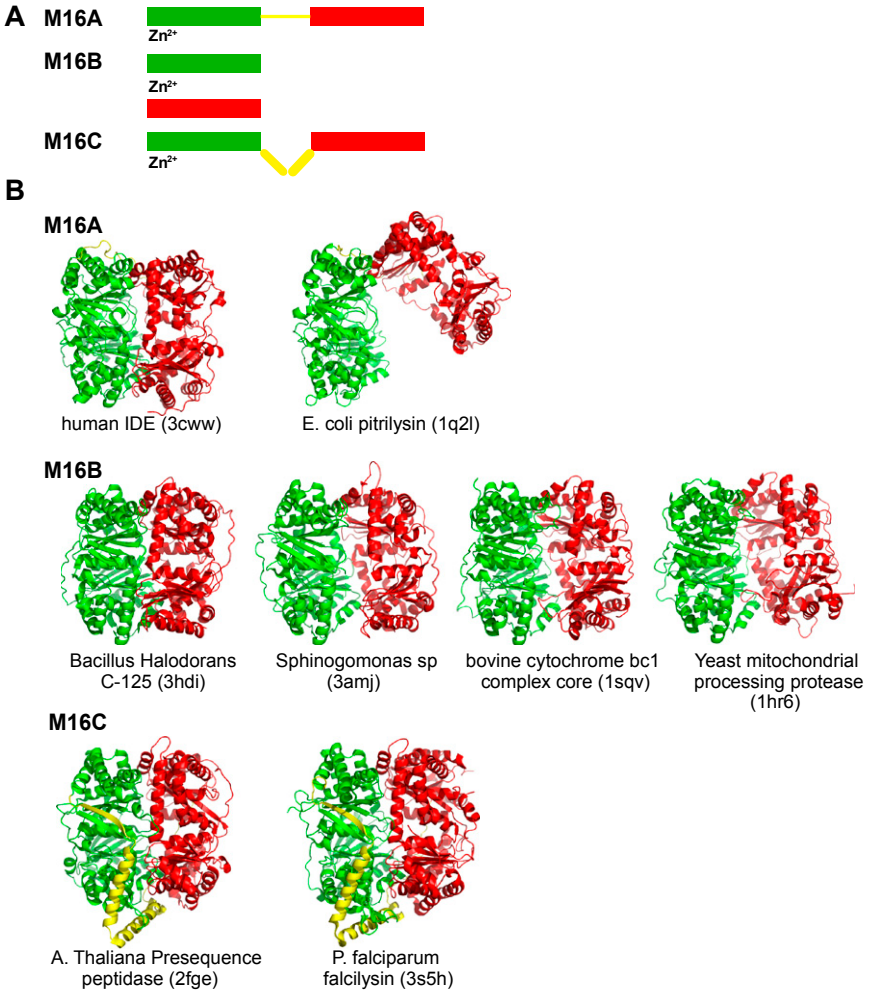

Fig. S1. M16 family. (*A*) Schematic diagram of M16A, M16B, and M16C protein. The green and red domains are roughly 45–50 kDa. In M16A and M16C, the green and red domains represent the N- and C-terminal halves of the metalloprotease joined by the linker (yellow). In M16B, these two domains are encoded by two different genes. (*B*) Structure comparison of the M16 family of proteases. Only representative structures with different degrees of opening between the two domains are shown, particularly for the M16B family.

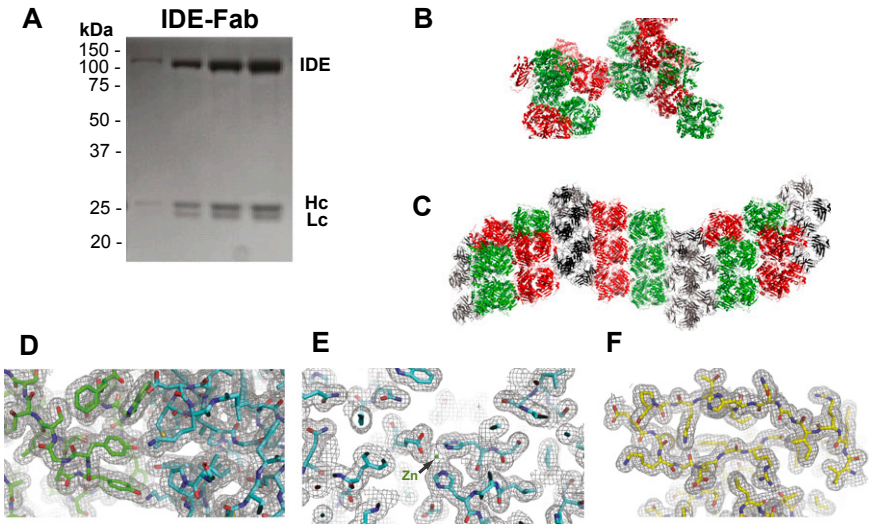

Fig. S2. Basic features of insulin degrading enzyme (IDE)-Fab$_{(IDE)}$ complex and crystal structure. (*A*) IDE and Fab$_{(IDE)}$ protein were incubated at an equal molar ratio and run on an S200 column, then subsequently electrophoresed by 15% SDS/PAGE conditions. Each lane presents a single band at ~110 kDa, representative of IDE, and a double band at 25 kDa, indicating the presence of the heavy (Hc) and light (Lc) chains forming a Fab$_{(IDE)}$ molecule. (*B* and *C*) Comparison of crystal packing of IDE dimer (*B*) with Fab$_{(IDE)}$-bound IDE dimer (*C*). Two IDE monomers in IDE dimer are colored as red and green, and two Fab proteins are shown as black and gray. (*D–F*) Electron density maps (2Fo-Fc at 1.0 σ) of representative regions of IDE-Fab$_{(IDE)}$, including the (*D*) IDE chain A (blue) and Fab heavy chain (green) binding interface; (*E*) IDE chain A catalytic region (blue; green, Zn^{2+} atom); and (*F*) IDE chain B (yellow) base subdomain.

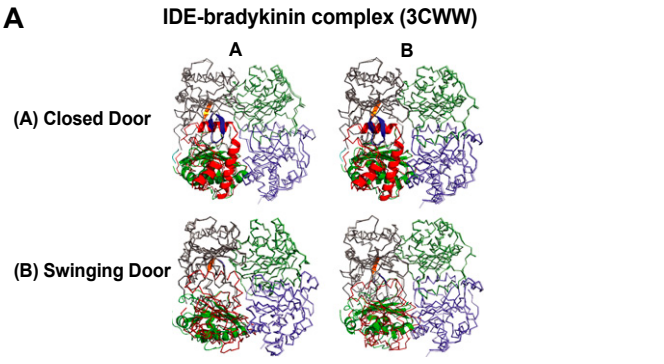

IDE (chain)	3CWW (A) (Å)	3CWW(B) (Å)	Average RMSD (Å)
(A) Closed	0.750	0.778	0.764
(B) Swinging Door	0.516	0.534	0.525

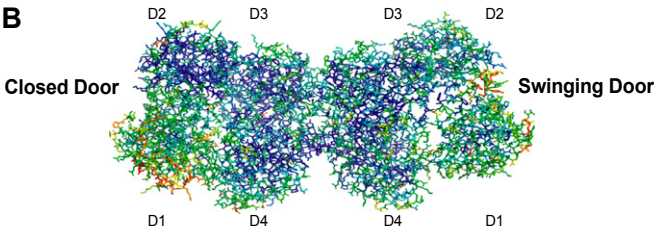

IDE (chain)	D1 (Å²)	D2 (Å²)	D3 (Å²)	D4 (Å²)	Overall B factor (Å²)
(A) Closed Door	76.8	44.4	41.6	49.1	52.8
(B) Swinging Door	70.3	59.6	41.8	46.7	53.0

Fig. S3. Overall structural analysis of IDE in IDE-Fab$_{(IDE)}$ complex. (*A*) Superimposition of chain A and B of IDE within IDE-Fab $_{(IDE)}$ with the closed door state of IDE (Protein Data Bank ID 3cww). (*B*) Thermal B factors of IDE D1-D4 domains in chain A and B of IDE.

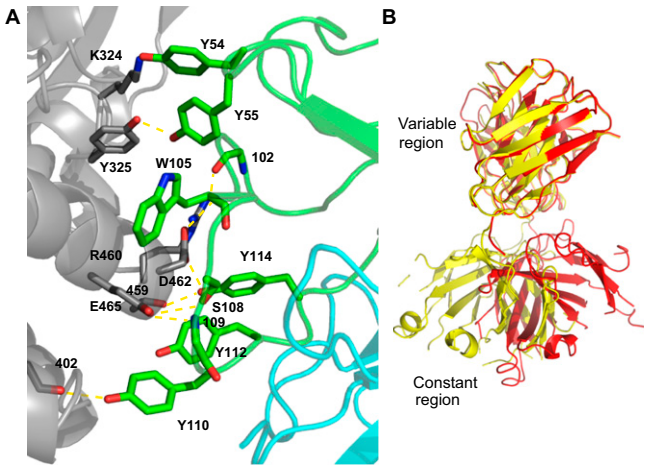

Fig. S4. IDE–Fab interaction. (*A*) Detailed interaction between the heavy chain of IDE-Fab with the D2 domain of IDE. The heavy and light chains of IDE-Fab are colored in green and cyan, respectively, and IDE D2 domain is shown in gray. (*B*) Superimposition of two IDE-Fab molecules, one that binds IDE closed door and one that binds IDE in the swinging door state, to reveal the rigid body movement of the constant region of two Fab molecules relative to the variable region.

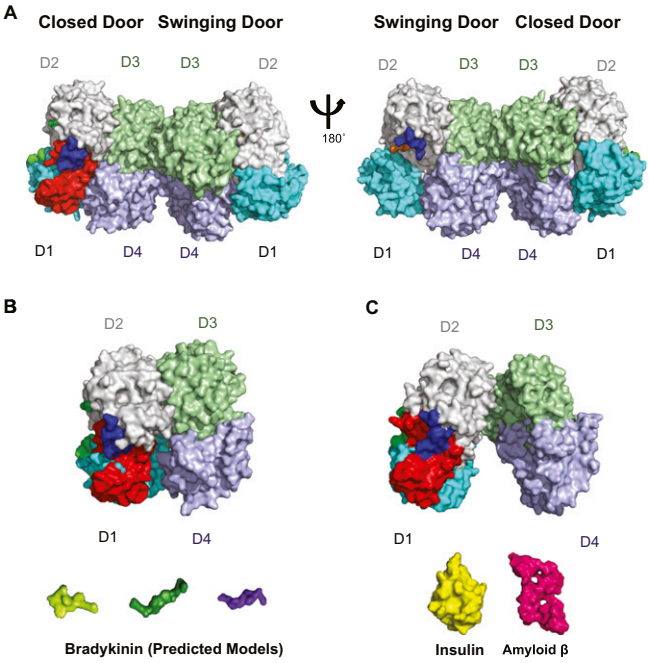

Fig. S5. Surface representation of IDE. (*A*) IDE dimer displaying the (*A*) closed door and (*B*) swinging door states. Dimer is rotated 180° to visualize the domain 1 (D1) differences between the two varying states. It is worth noting that the missing door subdomain in the swinging door state is not artificially incorporated into the representation in this figure when comparing with Fig. 2 *E* and *F*. We hypothesize that the door is present but disordered in our structure. Thus, IDE in the swinging door states has much smaller opening than what is depicted in this representation. (*B*) Putative door domain in the swinging door state is placed to show the 11- to 18-Å opening of the IDE catalytic chamber in the swinging door state, with three predicted models of bradykinin (helical, yellow; β-sheet, green; loop, purple) shown to illustrate potential small peptide degradation (i.e., bradykinin). (*C*) The D2/D3 pivot state of IDE, as predicted from small angle X-ray scattering (SAXS) data, is modeled to illustrate a catalytic chamber opening large enough to accommodate larger peptide degradation (i.e., insulin or amyloid β).

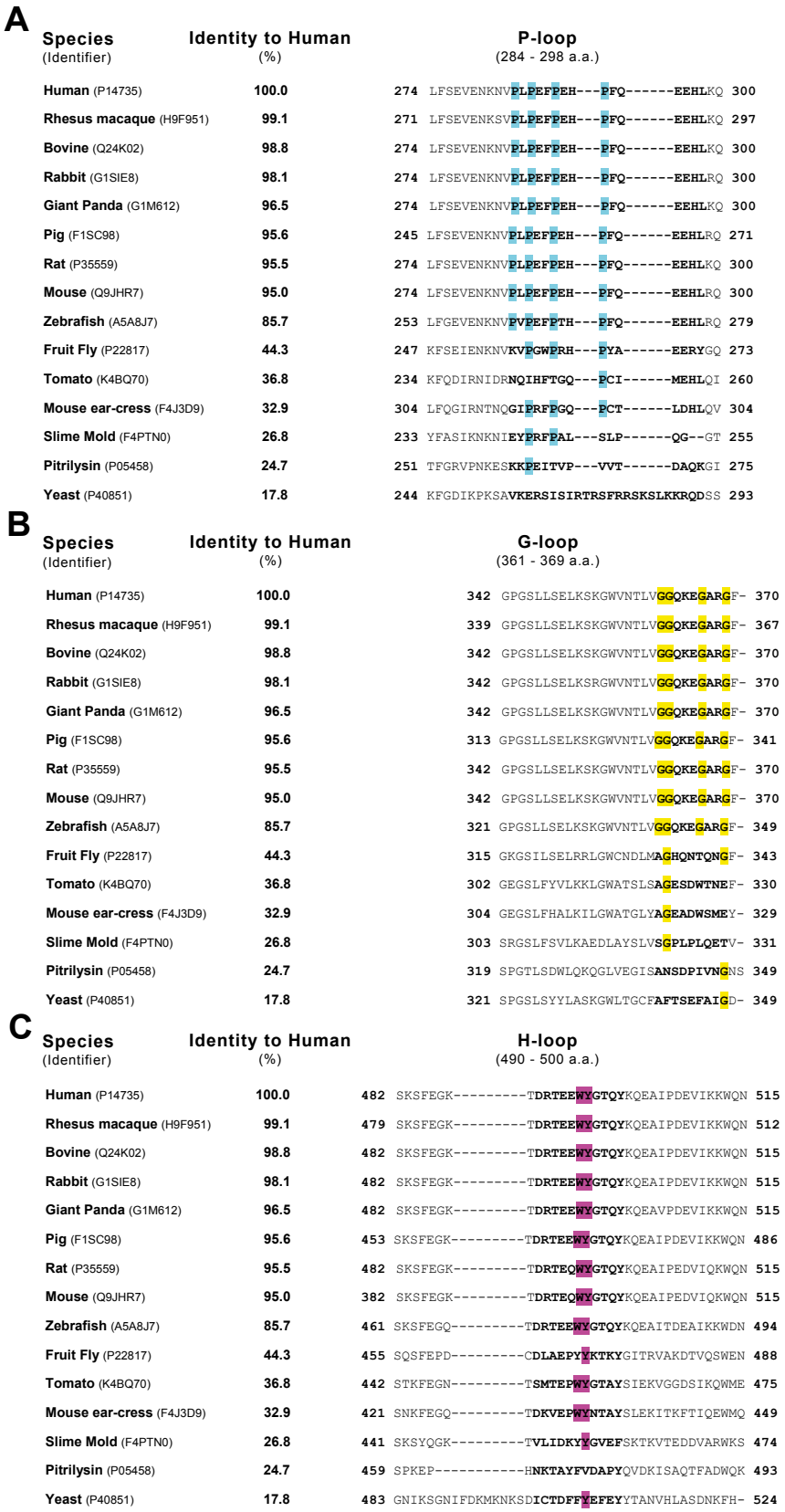

Fig. S6. Sequence alignment of IDE domain 1 subdomains for the proline-rich (P) loop (*A*), glycine-rich (G) loop (*B*), and hydrophobic residues at the tip (H) loop (*C*). The protein sequence ID of IDE homologs from mammals, insects, plants, fungi, and bacterium is indicated. Sequence identity is compared with human IDE. Each loop is shown by residues in bold font, whereas the conservation of particular residues is highlighted (blue, P-loop; yellow, G-loop; purple, H-loop).

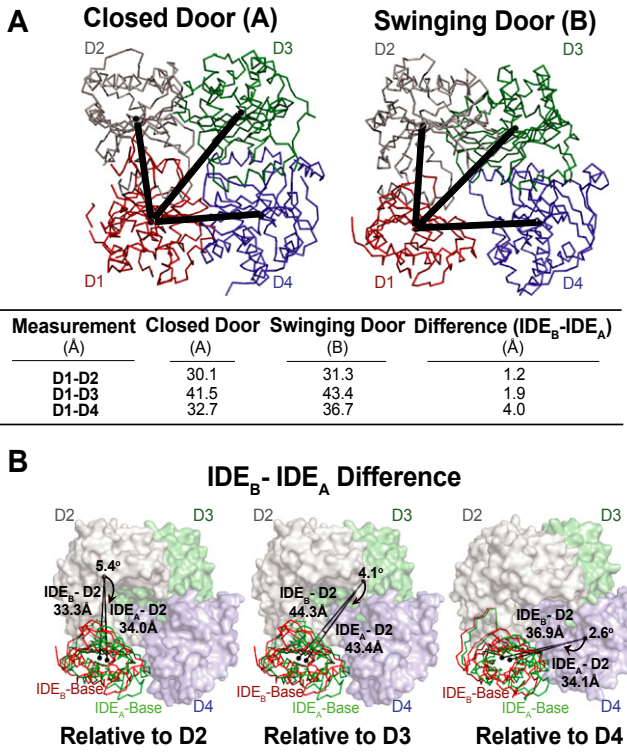

Measurement (Å)	Closed Door (A)	Swinging Door (B)	Difference (IDE$_B$-IDE$_A$) (Å)
D1-D2	30.1	31.3	1.2
D1-D3	41.5	43.4	1.9
D1-D4	32.7	36.7	4.0

Fig. S7. Measurements of rigid body movement of IDE base subdomain using the change in the center of mass (COM) of the base subdomain from COM of D2, D3, and D4 domains of IDE. (*A*) The COM of each domain and a measurement for length relative to domain 1 (D1) was calculated for the IDE (*A*) closed door and IDE (*B*) swinging door states. The measurement differences between the two states are recorded as the swinging door state minus the closed door state, IDE$_B$-IDE$_A$. (*B*) The swinging door state base was superimposed to the closed door state IDE chain, and the COM of the base for both IDE states was used to determine the difference in length and angle measurements relative to each of the D2, D3, and D4 domains.

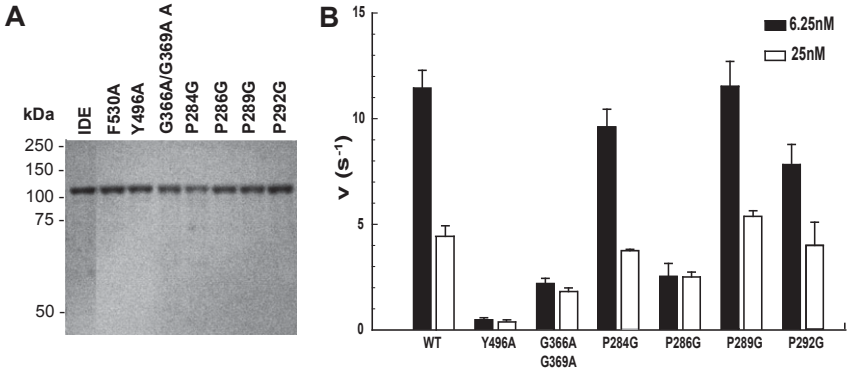

Fig. S8. Analysis of IDE purification and catalytic activities of IDE mutants. (*A*) IDE cysteine-free WT and mutant proteins were electrophoresed on 9% SDS/PAGE and subsequently stained by Coomassie Blue. Each lane represents 1 μg of fully purified protein, and each lane presents a single dominant band at ~110 kDa. (*B*) Relative activities of IDE (WT) and IDE mutants within the H-loop (Y496A), G-loop (G366A/G369A), and P-loop (P284G, P286G, P289G, P292G) at enzyme concentrations of 6.25 (black) and 25 (striped) nM. Activity was followed by measuring fluorescence resulting from the cleavage of 0.5 μM Substrate V at 37 °C. Background values were subtracted from experimental data and then plotted, a linear regression line was obtained for each respective protein at both concentrations (R^2 > 95%). The corresponding slope (m, y = mx + b), along with the maximum fluorescence reading for IDE at the end of the measurement and the concentration of substrate (500 pmol) and IDE (6.25 or 25 pmol), were used to calculate a specific activity. Data demonstrates mean ± SD from at least three experiments.

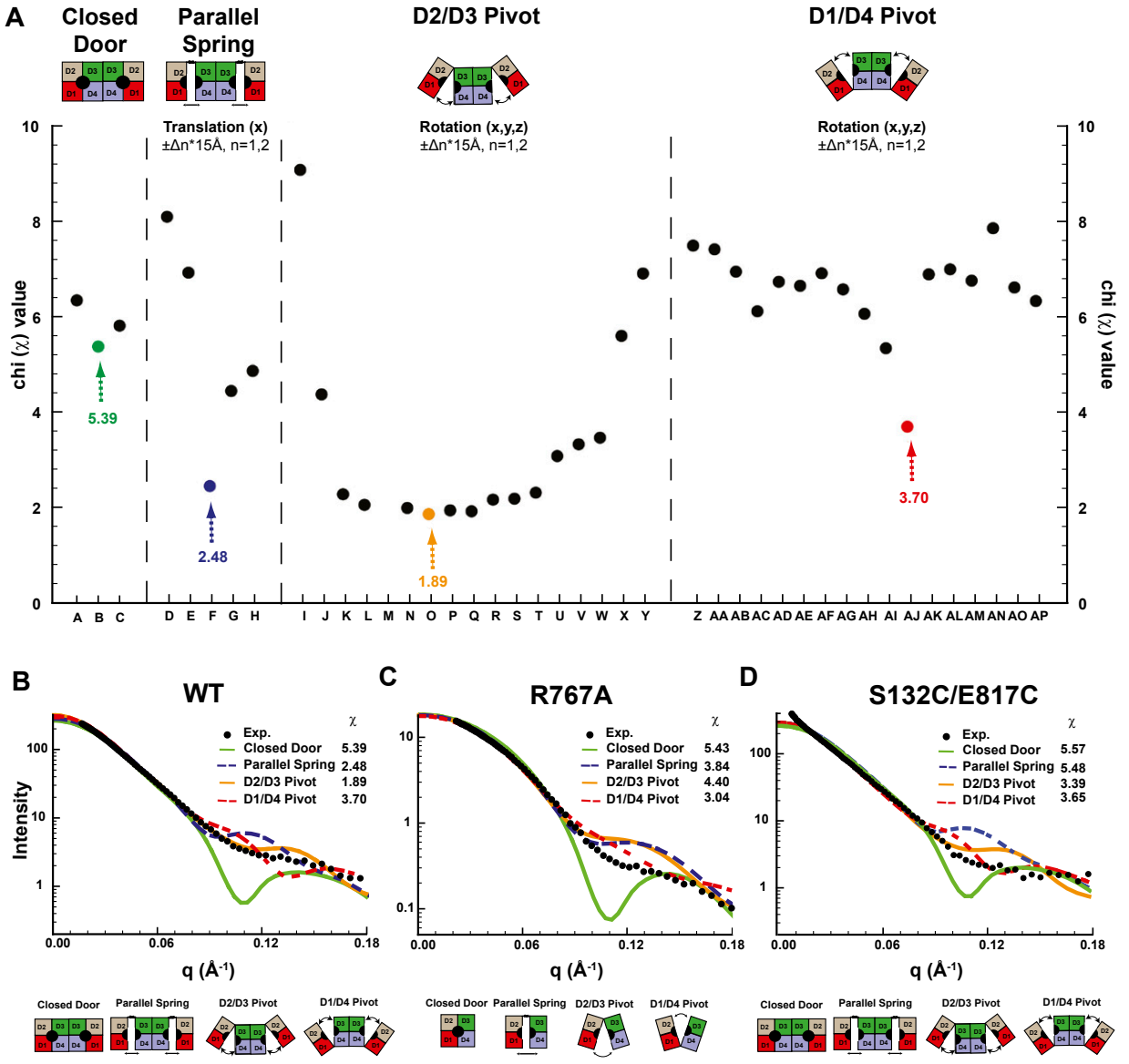

Fig. S9. SAXS Analysis of IDE and mutants in solution. (*A*) Proposed models of WT IDE in solution with altered degrees of openness, created using models of closed door or swinging door states (A–C), parallel spring with different degree of translation for the opening of the catalytic chamber (D–H), D2/D3 pivot with different rotations in the x, y, and z planes (I–Y), and D1/D4 pivot with different rotations in the x, y, and z planes (Z–AP). The lowest χ value, and thus highest statistical likelihood of fit, for each particular model is distinctly colored and was subsequently used for analysis. (*B–D*) SAXS scattering profiles of WT IDE (*B*), R767A (*C*), and S132C/E817C (*D*). Curve fitting is based on atomic models using the ATSAS CRYSOL program, such that black circles represent experimental data for IDE and solid lines display the various theoretical fits. WT IDE and S132C/E817C IDE, the disulfide bound cross-linked mutant, were fit using the dimer state with both chains in the respective model, whereas R767A IDE, the monomerized mutant, was fit using the proposed models in a monomer state. Chi values (χ) are shown to express the discrepancy between the experimental data and theoretical fits. A protein concentration of 1 mg/mL was used for the calculation of all scattering profiles, and the diagrams represent the proposed theoretical models of IDE in solution.

Table S1. Crystallographic statistics of IDE-Fab(IDE) complex

Variable	IDE-Fab
Crystallization condition	
IDE-Fab crystallized at 5 mg/mL	0.1 M sodium cacodylate, pH 6.5 0.2 M $MgCl_2$ 10% PEG-3000
Data collection	
Beam line	APS-19ID
Wavelength (Å)	0.9792
Space group	$P2_12_12_1$
Cell dimension (Å)	
a	56.96
b	131.65
c	377.02
α	90
β	90
γ	90
Resolution (Å)	50–3.36
Rsym (%)*	11.8 (68.8)†
I/sigma	14.1 (3.2)†
Redundancy‡	5.6 (5.6)†
Completeness (%)	99.9 (100)†
Unique reflections	41,849
Refinement	
R_{work}§	0.2322
R_{free}¶	0.2803
No. atoms	
Protein	20,933
rmsd	
Bond lengths (Å)	0.006
Bond angles (°)	1.578
Ramachandran plot (%)	
Favorable region	88.6
Allowed region	11.4
Generously allowed region	0
Disallowed region	0
Protein Data Bank ID	4IOF

*$R_{sym} = \Sigma_j|\langle I\rangle - I_j|\Sigma\langle I\rangle$, where I_j is the intensity of the j[th] reflection and $\langle I \rangle$ is the average intensity.

†Outer resolution shell.

‡N_{obs}/N_{unique}.

§$R_{work} = \Sigma_{hkl}|F_{obs} - F_{calc}|/\Sigma_{hkl} F_{obs}$.

¶R_{free}, calculated the same as R_{work}, but on the 5% data excluded from refinement calculation.